Amplitude-Coherent Detection for Optical Wireless Communications: Opportunities and Limitations

Mohammad A. Al-Jarrah, *Member, IEEE,* Arafat Al-Dweik, *Senior Member, IEEE,*, Ki-Hong Park, *Member, IEEE,* and Mohamed-Slim Alouini, *Fellow, IEEE*

***Abstract*—The proliferation of ubiquitous computing applications created a multi-dimensional optimization problem that includes several conflicting variables such as spectral efficiency, complexity, power consumption, delay, and error probability. To relax the problem and provide efficient solutions, it was necessary to augment the currently overutilized radio spectrum with new frequency bands such as the optical spectrum, which can be used to off-load some of the traffic of certain applications. Therefore, this paper presents an efficient system design that uses amplitude-coherent (AC) detection to reduce OWC system's complexity, improve its reliability and spectral efficiency. More specifically, we use amplitude shift keying with orthogonal frequency division multiplexing (OFDM) at the transmitter, and AC detection at the receiver. The complexity reduction is achieved by using a low complexity detector, channel estimator, and peak-to-average power ratio (PAPR) reduction scheme. The spectral efficiency is achieved by using real data symbols with discrete cosine transform (DCT), which requires a subcarrier spacing that is 50% of the discrete Fourier transform (DFT), and does not require Hermitian symmetry to generate real-valued OFDM signals. Moreover, the derived channel estimator is blind, and the PAPR reduction scheme does not require a feedback overhead between the transmitter and receiver.**

***Index Terms*—Optical communications, visible light communications, free space optics, OWC, VLC, FSO.**

I. Introduction

Optical wireless communications (OWC) use unguided visible, infrared (IR), or ultraviolet (UV) light to carry information. Based on the operating wavelength, OWC can be classified as visible light communications (VLC), free space optical (FSO), or ultraviolet communication (UVC). VLC (390-750 nm) systems use light emitting diodes (LEDs) which can be pulsed at very high speeds without noticeable flicker effect on the human eye. VLC can be used in various applications such wireless local area networks, wireless personal area networks, and vehicular networks. FSO (750-1600 nm) is typically used for terrestrial point-to-point communications where laser transmitters are used to provide low cost links with high data rates. FSO is considered as an efficient solution for the backhaul bottleneck. UVC (200-280 nm) have some inherent advantages such as the low background solar radiation, low device dark noise, and less restrictive requirements for pointing [1]. UVC is used in applications such as aircraft landing aid under low visibility atmospheric conditions, missiles plume detection, and tactical battlefield.

One of the main features of OWC is its ability to offer very high bandwidth, which may allow the transmission of very high data rates. For example, Tsonev *et al.* [2] demonstrated a VLC system using a single 50-μm gallium nitride LED that can offer a data rate of 3 Gb/s. FSO can generally support much higher data rates as demonstrated in [3]. UVC data rates are generally much less than VLC and FSO links, particularly for long distances. For example, Puschell and Bayse [4] demonstrated a UVC link with 1.2 Mbps over 1.6 km distance while the authors in [1] demonstrated an experiment with data rates of 71 Mbps for very short distance such as 8 cm.

M. A. Al-Jarrah is with the School of Electrical and Electronic Engineering, University of Manchester, Manchester M13 9PL, U.K. (Email: mohammad.al-jarrahat@postgrad.manchester.ac.uk)

A. Al-Dweik is with the Center for Cyber Physical Systems, Khalifa University, Abu Dhabi, UAE. (E-mail: arafat.dweik@ku.ac.ae). Also, he is with the Department of Electrical and Computer Engineering, Western University, London, ON, Canada. (E-mail: dweik@fulbrightmail.org)

K.-H Park and M.-S. Alouini are with King Abdullah University of Science and Technology (KAUST), Thuwal, Makkah Province, Kingdom of Saudi Arabia, (E-mail: {kihong.park, slim.alouini}@kaust.edu.sa)

A. OWC Modulation Schemes

Although OWC spectrum is in the order of 100s of Terahertz, there are several challenges that limit high data rate transmission, with reasonable cost and complexity. Typically, the main limitation for achieving high data rates is the availability of hardware that can support such high rates. In VLC, for example, the modulation response for commercially available LEDs can be as low as few MHz, and with the application of blue filter at the receiver side can increase to 20 MHz [2]. Even with the use of fast LEDs that can have up to 60 MHz bandwidth [2], the utilized bandwidth remains very limited as compared to the available one. Consequently, using spectral and energy efficient modulation schemes remains crucial to design reliable and cost-efficient OWC systems. It is worth noting that the IEEE 802.15.7 standard proposes on-off keying (OOK), variable pulse-position modulation (VPPM), and color-shift keying (CSK) as modulation techniques for indoor VLC systems. In this standard the highest data-rate envisaged is 96 Mbps for OOK and CSK, or 24 Mbps for VPPM.

In the literature, a wide range of modulation schemes have been investigated for OWC, a comprehensive survey can be found in [5]. Generally speaking, the considered modulation schemes can be classified as single or multi-carrier, coherent or noncoherent, multi-level or binary. A particular combination from these options determines the system spectral efficiency, energy efficiency, complexity, and error rate. Nevertheless, regardless of the selected modulation scheme, the resulted signal should be positive and real when intensity modulation and direct detection (IM-DD) are considered. Using multicarrier techniques such as orthogonal frequency division multiplexing (OFDM) can improve the spectral efficiency of OWC [2], however the energy efficiency is not high due to the peak-to-average power ratio (PAPR) problem, which requires high DC bias values to avoid clipping the negative part of the OFDM signal [6], [7]. Moreover, the spectral efficiency of OFDM when used in OWC with IM-DD is less than what is expected with radio frequency (RF) applications, which is due to the fact that OFDM signals have to be real and positive. For example, in DC biased optical OFDM (DCO-OFDM), only 50% subcarriers may carry information, while it is about 25% for asymmetrically clipped optical OFDM (ACO-OFDM). The high PAPR may also introduce positive peaks clipping effects as the practical LEDs have the typical nonlinear characteristics.

B. OWC Channel Impairments

The channel behavior for OWC depends on several factors such as the characteristics of the hardware, distance between the transmitter

and receiver, and weather the system is indoor or outdoor. In the literature, the performance of OWC has been investigated using non-fading and fading channel models. The typical fading models are the log-normal, Gamma-Gamma, Rice, negative exponential, and I-K fading, and additive white Gaussian noise (AWGN) is used to model the receiver noise [5]. The frequency-selectivity and coherence time are important considerations for OWC. For FSO links, the channel delay spread is usually negligible even in severe atmospheric conditions. However, the channel coherence time is very large which implies that the signal might go into a deep fade for periods of time that span thousands of symbols. For VLC, the channel may exhibit frequency selectivity due to the light reflections from walls and other objects [9]. Phase noise and I/Q imbalance are other factors that affect the error performance of OWC systems when coherent modulation schemes are adopted [10].

C. Work Motivation

As can be noted from the surveyed literature, using higher order modulation combined with OFDM may have several advantages for OWC. However, the spectral efficiency, PAPR, phase noise, I/Q imbalance and channel state information (CSI) estimation errors are among the main limitations. Therefore, we consider in this work using amplitude-coherent (AC) detection, also known as semi-coherent detection [11]–[13] for OWC to jointly resolve some of the main limitations inherent to conventional optical OFDM systems. The AC detection relaxes the requirements for the channel estimation process, enables low complexity blind channel estimation and PAPR reduction, and has immunity to phase noise and I/Q imbalance. Moreover, OFDM spectral efficiency can be enhanced by using the inverse discrete cosine transform (IDCT) and DCT for data modulation and demodulation, respectively, where using the DCT with one-dimensional data symbols enables avoiding the Hermitian symmetry constraint [14]. OFDM with DCT/IDCT will be denoted as C-OFDM, while conventional OFDM using the Fourier transform will be denoted as F-OFDM.

II. Amplitude-Coherent detection for Optical OFDM

When AC detection is adopted, the data symbols should be modulated using unipolar M-ary amplitude shift keying (ASK) [12]. Given that the channel fading is flat, then the received signal in general can be described as $r = hs + n$, where s is the ASK information symbol selected uniformly from a one-dimensional unipolar constellation $\{d_0, d_1, \ldots, d_{M_A-1}\}$, h is the channel coefficient and n is the AWGN. Given that only the channel power gain $|h|^2 \triangleq \omega$ is available at the receiver, the data symbols can be efficiently extracted by equalizing the energy of r, i.e., $|r|^2$, using ω. Then, a simple threshold detector can be used, which corresponds to the heuristic AC detector [12].

Generating an OFDM signal using ASK symbols can be performed efficiently using the IDCT at the transmitter side [14], [15]. By noting that the data and transform matrix elements have real values, then the IDCT output is real as well, and hence, the Hermitian symmetry constraint is not required for C-OFDM. However, the IDCT output is not necessarily positive, and thus, DCO-OFDM or ACO-OFDM can be used [7] to generate strictly positive OFDM signals. Nevertheless, ACO-OFDM is considered in this work. Because Hermitian symmetry is not required for C-OFDM, the number of modulated subcarriers in an N-point IDCT is $N/2$, because only odd subcarriers are modulated.

Given that the channel fading is flat over at least one OFDM symbol, the received signal after DCT and dropping the even subcarriers can be written as $\mathbf{r} = h\mathbf{s} + \mathbf{n}$, where $\mathbf{r}$, $\mathbf{s}$ and $\mathbf{n}$ are $(N/2) \times 1$ vectors, N is the total number of subcarriers. The data symbols are then extracted using the heuristic AC detector [11]–[13].

A. Spectral Efficiency

Based on the modulation type, three different OFDM configurations can be obtained. For fair comparison, we assume that all systems use ACO-OFDM. The three types are:

1) If two-dimensional modulation schemes such as quadrature amplitude modulation (QAM) are used, then the OFDM can be generated by applying the inverse fast Fourier transform (IFFT) at the transmitter. Given that the OFDM symbols consists of N subcarriers produced using N-point IFFT, and N_Q is the effective number of modulated subcarriers, then the spectral efficiency $\eta_Q \triangleq N_Q \log_2(M_Q)/B_Q$, where M_Q is the modulation order and B_Q is the bandwidth. For F-OFDM $B_Q \approx N/T$ [15], where T is the symbol period, which can be normalized to one. For ACO-OFDM, only the odd subcarriers transmit data symbols, and the data vector should be Hermitian symmetric. Therefore, $N_Q = N/4$, and $\eta_Q = 0.25 \log_2(M_Q)$.
2) If bipolar ASK ($\overline{\text{ASK}}$) is used, then additional spectral efficiency can be achieved by using the C-OFDM. By noting that the IDCT has subcarrier spacing of $1/2T$ and the Hermitian symmetry constraint is waived, the number of modulated subcarriers $N_{\bar{A}} = N/2$, and the bandwidth $B_{\bar{A}} \approx N/2T$ for $N \gg 3$ [15]. Therefore, the spectral efficiency $\eta_{\bar{A}} = \log_2(M_{\bar{A}})$, where $M_{\bar{A}}$ is the modulation order of the $\overline{\text{ASK}}$ symbols.
3) For unipolar ASK (ASK) symbols that can be used for AC detection, the number of modulated subcarriers $N_A = N/2$, and the bandwidth is similar to the $\overline{\text{ASK}}$ case. Therefore, $\eta_A = \log_2(M_A)$, where M_A is the modulation order of the unipolar symbols.

For the three systems to have equal spectral efficiency, i.e., $\eta_Q = \eta_{\bar{A}} = \eta_A$, then the modulation orders should be selected such that $M_{\bar{A}} = M_A = \sqrt[4]{M_Q}$. Under the equal spectral efficiency constraint, each of the three configurations may have different modulation order, and hence different receiver complexity, bit error rate (BER), PAPR, and sensitivity to RF imperfections. For example, using 2-$\overline{\text{ASK}}$ is more desirable than a 16-QAM because it offers advantages in all aspects. The ASK can use the same modulation order, and hence, $\overline{\text{ASK}}$ will have better BER performance, but it will have higher receiver complexity due to the channel estimation needed for the coherent detection, and PAPR reduction process. Moreover, $\overline{\text{ASK}}$ is more sensitive to RF impairments.

B. Bind Channel Estimation

CSI estimation is necessary to recover the information symbols coherently. In most practical systems, pilot symbols are ingrained within the data sequence $\mathbf{s}$ to enable the estimation of h. In flat fading channels, the estimation error can be reduced by averaging over multiple pilot symbols. Nevertheless, pilot symbols do not carry information and hence, they deteriorate the spectral efficiency.

When AC detection is adopted, the detector requires the knowledge of ω to extract the data symbols reliably, i.e., it does not require the channel phase. Given the all data symbols in $\mathbf{s}$ are equally probable, then the average number of symbols with a particular amplitude is $N/(2M_A)$. For example, in the binary case $M_A = 2$, $d_0 = 0$, $d_1 = \sqrt{2}$, thus on average, there are $N/4$ symbols modulated using d_0 and $N/4$ symbols using d_1. At high signal to noise ratios (SNRs), the energies $|r_i|^2$ that correspond to d_1 symbols are most likely to be larger than the energies for d_0 symbols. Consequently, choosing $L \leq N/4$ samples with the maximum amplitudes among the $N/2$ modulated subcarriers implies that we roughly managed to identify

Algorithm 1: PAPR Reduction using Bit-Flipping

Input: $\mathbf{p}^1$, $\mathbf{s}$, I
Output: $\mathbf{p}$

for $i = 2$ **to** I
  for $v = 1 : 2 : N-1$
    if $p_v^i = 0$
      Go to 14
    end
    $\beta_1 = \text{PAPR}\left(\mathbf{s} \circ \mathbf{p}^i\right)$
    $p_v^i = -p_v^{i-1}$ (Bit flipping)
    $\beta_2 = \text{PAPR}\left(\mathbf{s} \circ \mathbf{p}^i\right)$
    if $\beta_1 < \beta_2$
      $p_v^i = p_v^{i-1}$
    else
      $p_v^i = -p_v^{i-1}$
    end
  end
end
$\mathbf{p} = \mathbf{p}^I$

L subcarriers whose data symbols are d_1. Given that the set of the maximum L amplitudes is denoted as $\mathbb{L}$, then ω can be estimated as

$$\hat{\omega} = \frac{1}{2L} \sum_{l \in \mathbb{L}} |r_l|^2 . \tag{1}$$

For large values of L, the ensemble average approaches the statistical average, which implies that $\hat{\omega} \approx \omega$. The same approach can be applied for the case where $M_A > 2$.

III. PAPR Reduction using bit-flipping algorithm

PAPR is one of the main limitations for OFDM systems, and it is more critical for unipolar ASK constellations because all symbols have the same polarity. The PAPR can be reduced by changing the phase of the data symbols using a predetermined sequence $\mathbf{p} = [p_0, p_1, \ldots, p_{N-1}]$, $p_i \in \{1, 0, -1\}$, thus, the signal applied to the IDCT is $\mathbf{g} = \mathbf{s} \circ \mathbf{p}$, where '$\circ$' denotes the Hadamard product. Generating the optimum phase sequence requires $2^{N/2}$ trials, which is prohibitively expensive. Therefore, we propose a suboptimal heuristic algorithm, **Algorithm 1**, to compute $\mathbf{p}$ efficiently. Initially, a random version of $\mathbf{p}$ is generated offline, denoted as $\mathbf{p}^1$. If no additional iterations are desired, then $\mathbf{g} = \mathbf{s} \circ \mathbf{p}^1$, otherwise, **Algorithm 1** is called to optimize $\mathbf{p}^1$ iteratively. In each iteration, the PAPR of the OFDM symbol is tested given $\mathbf{p}^i$, and then it is computed again after flipping the polarity of the first bit in $\mathbf{p}^i$, the final bit polarity is the one that provides less PAPR. Once the bit value is decided, it remains fixed to the end of the iteration. The process is repeated for all other bits in $\mathbf{p}^i$ using the same approach. Therefore, **Algorithm 1** is called the bit-flipping algorithm, and it can be noted that it is a greedy algorithm within each iteration. The same process is repeated for all consequent iterations. In addition to its low complexity, the proposed algorithm does not require to send any information to the receiver about the sequence $\mathbf{p}$, because the phase information is irrelevant for AC detection.

IV. Complexity Analysis

The complexity of the proposed C-OFDM and conventional F-OFDM is mostly determined by the modulation/demodulation operations, PAPR reduction scheme, CSI estimation, and data detection. Therefore, each of these subsystems is discussed and compared to conventional F-OFDM. The computational complexity is derived assuming that the FFT and fast cosine transform (FCT) are adopted.

A. Modulation-Demodulation

1) **F-OFDM:**

- The OFDM symbol generation at the transmitter and data extraction at the receiver requires the computation of an IFFT and FFT, respectively. Computing an N-point FFT or IFFT using efficient algorithms such as the radix-2 Cooley-Tukey algorithm requires $\mathcal{N}/2$ complex multiplications, where $\mathcal{N} = N \log_2 N$, and $\mathcal{N}$ complex additions. By noting that each complex multiplication is equivalent to three real multiplications and three real additions, and each complex addition is equivalent to two real additions, the total number of real multiplication and addition operations required for the IFFT plus FFT is $3\mathcal{N}$ and $10\mathcal{N}$, respectively.
- After FFT at the receiver, the data subcarriers are extracted where even and Hermitian symmetry subcarriers are discarded. The complexity of this operation is generally negligible because the subcarrier allocation is fixed.
- The subcarriers that carry information will be equalized using zero-forcing using an estimated version of the channel coefficient. The complexity of the channel coefficient estimation is discussed in subsection II-B. The information symbols can be extracted from the soft samples after equalization using a maximum likelihood detector (MLD). The complexity of the equalization process and MLD for a QAM symbol requires $6M_Q$ real multiplications and $5M_Q$ real additions per symbol. Therefore, the total complexity for the MLD process for all subcarriers is significant, particularly for large modulation orders.

2) **C-OFDM:**

- For the FCT, all operations are real where the total number of real multiplications and additions is $0.5\mathcal{N}$ and $1.5\mathcal{N} - N + 1$, respectively [15]. Therefore, the total IFCT plus FCT operations are $\mathcal{N}$ real multiplications and $3\mathcal{N} - 2N + 2$ real additions. Consequently, the number of real multiplications for the F-OFDM is three times larger than the C-OFDM, and the real additions are more than seven times larger.
- After the FCT, the odd subcarriers are extracted, and similar to the F-OFDM case, the complexity of this step is negligible.
- The energy for each sample is then computed, which requires two real multiplications and one real addition for each data subcarrier.
- The equalization process requires only one real division, which is simpler than F-OFDM case. The complexity of the channel estimation is given in subsection II-B.
- Unlike coherent QAM, AC detection can be performed efficiently using the heuristic AC detector [11]–[13].

It is also worth noting the complexity difference between the detectors of the two configurations. In the case that the two configurations are using the same modulation order, then the complexity of the two detectors is generally equivalent. However, under equal spectral efficiency constraints, the modulation order of the F-OFDM is much larger, and hence, the complexity of the MLD is much higher as well.

B. PAPR Reduction

The proposed PAPR reduction complexity can be summarized as follows:

1) Compute $\mathbf{g} = \mathbf{p}^1 \circ \mathbf{s}$, the complexity of this process is negligible because it only requires flipping the signs of the non-zero elements in $\mathbf{s}$. If signed integer representation is used, then flipping the phase requires simply inverting one bit.
2) For each non-zero bit, flip the bit value and compute the IFCT using the updated bit value. Given that $x_m^i|p_v^i$ is the mth sample at the IFCT output computed using p_v^i during the ith iteration, then $x_m^{i+1}|p_v^{i+1}$ can be computed as
$$x_m^{i+1}|p_v^{i+1} = x_m^i|p_v^i - p_v^i \times 2\cos\left(\frac{\pi v\,[2m+1]}{2N}\right) \quad (2)$$
which is due to the fact that $p_v = \pm 1$. Moreover, the term $2\cos(\pi v\,[2m+1]/2N)$ can be computed one time off-line, and the value of p_v can be used to control the signs of its elements. As a result, for each non-zero bit we need to compute N real subtractions, and thus, $(I-1) \times N^2/4$ real subtractions for each OFDM symbol, but no multiplications are required. It is worth noting that capturing the signal peak accurately requires oversampling the IFCT output, which can be achieved using a zero-padded data vector, which also increases the size of the IFCT. Nevertheless, the IFCT complexity scales linearly with the oversampling factor Q due to the sparseness of the oversampled data vector.
3) Computing the PAPR typically requires calculating
$$\frac{\max\{x_m^2\}}{\sum_m x_m^2}, \forall x_m \neq 0. \quad (3)$$
Because the data samples are real, each squaring process requires only one real multiplication. However, it should be noted that after zero-clipping, the OFDM signal becomes positive, further to being real. Consequently, the PAPR reduction can be achieved by minimizing $\max\{x_m\}/\sum_m x_m$, which has much lower computational complexity when compared to the conventional PAPR, because no multiplication operations are required. Monte Carlo simulation results confirmed that using either metric would result in the same PAPR reduction value.

The complexity of PAPR reduction of the F-OFDM is determined by the algorithm used. For example, if the partial transmit sequence (PTS) is used, then we have to search for the best phase sequence that will be used, and in each search iteration a QN-point IFFT should be computed V times, where V is the number of partitions, typically more than 16. Given that the phase sequence used is binary, then at least $V+1$ iterations are needed. Consequently, the complexity of the proposed PAPR reduction algorithm is substantially less complex than the algorithms used for F-OFDM with QAM symbols.

C. Channel Estimation

As can be noted form Section II-B, CSI estimation can be divided into three main steps:

1) Compute $|r_i|^2 \triangleq \gamma_i$ for all data samples at the DCT output, however, these value are needed for the detection process, and hence their complexity is already considered as a part from the detection process.
2) Select the maximum L values from $\{\gamma_1, \gamma_3, \ldots, \gamma_{N-1}\}$, which presumably correspond to L samples where symbol d_{M_A-1} is transmitted. The value of L should be selected to minimize the mean-square error (MSE). Given that the transmitted symbols are equiprobable, then the average number of symbols whose value is d_{M_A-1} would be $N/(2M_A)$. Consequently, if $L \gg N/(2M_A)$, then several samples where $d_i \neq d_{M_A-1}$ will be included, which may deteriorate the MSE, and using $L \ll N/(2M_A)$ implies that several useful samples are not utilized, which may affect the MSE as well. Therefore, the size of L should be optimized to minimize the MSE. Nevertheless, Monte Carlo simulation results revealed that using $L \geq 16$ is sufficient to provide BERs that are equivalent to those obtained using perfect channel estimates. Therefore, we consider a fixed L in this work while deriving the optimum L will be considered in our future work. Furthermore, because we do not strictly require the maximum L elements, lower and faster algorithms can be developed. For example, the L samples can be selected by comparing γ_i to a certain threshold, which may significantly reduce the time and space requirements. The complexity of the sorting process is usually evaluated in terms of time and space, and thus, cannot be evaluated in terms of number of mathematical operations. A special case of interest is for the 2-ASK scenario, where it can be demonstrated that ω can be estimated accurately using all data samples. Therefore, a significant complexity reduction can be obtained by eliminating the search for the maximum L values. Such result is obtained because the samples modulated using d_0 have very limited effect on the estimation accuracy, even if they are included in the estimation process.
3) Compute the estimated $\hat{\omega}$ as described in Section II-B which has $R_A = 2L+1$, $R_M = 2$, and $R_D = 2$, where R_D denotes the real divisions.

Therefore, the overall computational complexity of the proposed channel estimation algorithm is fairly low. Comparing the proposed algorithm to the conventional least-square estimation using pilot symbols, it can be noted that choosing the maximum L symbols is the only additional operations required. However, the proposed algorithm is blind because no pilot symbols are required.

V. Numerical Results

The section presents the numerical results for an OFDM based OWC system where the number of subcarriers $N = 64$ and the three system models are considered, which are the C-OFDM with ASK and $\overline{\text{ASK}}$ modulation, and F-OFDM using QAM. The results are generated given that all systems have the same spectral efficiency, and hence, two groups of modulation orders are used $\mathbf{m}_1 = [2, 2, 16]$ and $\mathbf{m}_2 = [4, 4, 256]$, where the elements of $\mathbf{m}$ represent the modulation orders of the M_A, $M_{\bar{A}}$ and M_Q, respectively. All the considered systems are implemented as ACO-OFDM, and thus, the data is transmitted on the odd subcarriers while even subcarriers are nulled. For the F-OFDM, the Hermitian symmetry is considered, while it is not applied for the C-OFDM because the data and transform are real. The negative part of the signals is clipped at the zero level, and different clipping levels are used for the positive signals. The $\overline{\text{ASK}}$ and QAM symbols are recovered using a coherent MLD while ASK symbols are recovered using the heuristic AC detector. A flat fading channel with Gamma-Gamma distribution is considered where $\alpha = 8$ and $\beta = 6$, and thus, the Rytov variance (scintillation index) $\sigma_{\text{R}} = 0.3125 > 0.3$, which corresponds to a moderate turbulence environment. Monte Carlo simulation is performed using 10^5 realizations for each simulation point. The detection for all types of modulation schemes is performed while considering perfect CSI, unless it is stated otherwise.

Fig. 1 shows the complementary cumulative distribution function (CCDF) of the PAPR for the considered systems using $\mathbf{m}_1$ scenario.

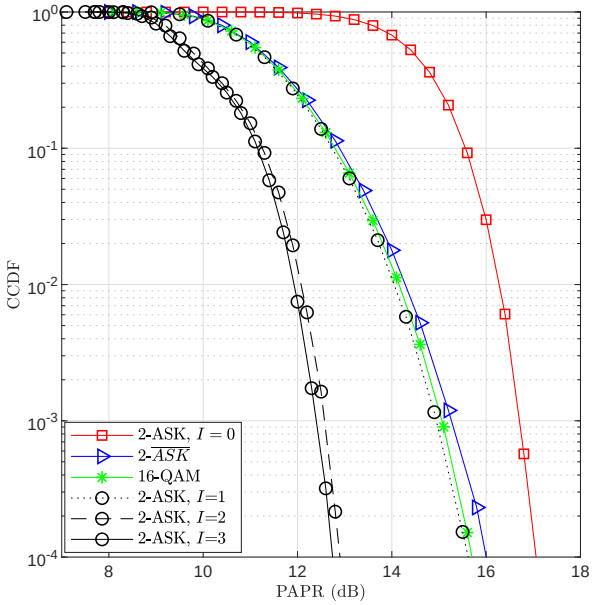

Fig. 1. CCDF for the considered modulation schemes, the ASK is considered with and without PAPR reduction.

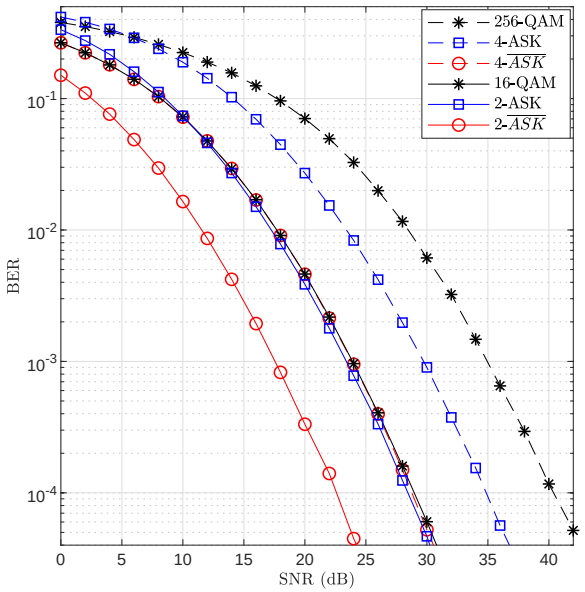

Fig. 2. BER for different detection methods and different values of M.

The PAPR is measured after zero-clipping, which actually increases the PAPR for all systems by 3 dB. The 2-ASK is considered with and without the proposed PAPR reduction algorithm while the other modulation schemes are considered without PAPR reduction. As can be noted from the figure, the PAPR of the 2-ASK without PAPR reduction is higher than all the other considered systems, which makes it the most susceptible to the system nonlinearity. Using **Algorithm 1** with one iteration reduced the PAPR by about 1 dB at CCDF of 10^{-4}, which makes it comparable to the PAPR of 2-$\overline{\text{ASK}}$ and 16-QAM cases. Using one additional iteration managed to provide an additional 3 dB of PAPR reduction as compared to the case with a single iteration. However, the PAPR reduction achieved by increasing the number of iterations to three provided only an additional 0.25 dB. Therefore, using $I > 2$ provides negligible additional PAPR reduction.

Fig. 2 shows the BER that can be achieved at the receiver by applying different detection methods using $\mathbf{m}_1$ and $\mathbf{m}_2$. The transmitter is assumed to have linear amplifier and LED, and hence, positive clipping is not considered. For the $\mathbf{m}_1$ scenario, the 2-$\overline{\text{ASK}}$ offers the best performance as expected, followed by the 2-ASK, and then 16-QAM. The 2-ASK has moderate BER where there is about 6 dB loss at 10^{-4} as compared to the 2-$\overline{\text{ASK}}$, while the 2-ASK and 16-QAM have comparable BER. For the $\mathbf{m}_2$ scenario, the same trend is maintained, except that the 4-ASK outperforms the 256-QAM by about 6 dB at BER of 10^{-4}. It is also worth noting that the 2-ASK, 4-$\overline{\text{ASK}}$ and 16-QAM have comparable BER.

Fig. 3 presents the BER for the considered schemes using $\mathbf{m}_2$ where a positive clipping level $\mu_c = 1.5$ is applied. The ASK is considered with PAPR reduction using different number of iterations, and the case where $I = 0$ indicates that no PAPR reduction is utilized. The figure clearly shows that 4-ASK without PAPR reduction and 256-QAM perform very poorly with high BER floors for the considered SNR range. The 4-$\overline{\text{ASK}}$ performs well at low SNRs because the performance in this range is dominated by the AWGN, however at high SNRs, the BER is dominated by the inter-carrier interference (ICI) caused by the

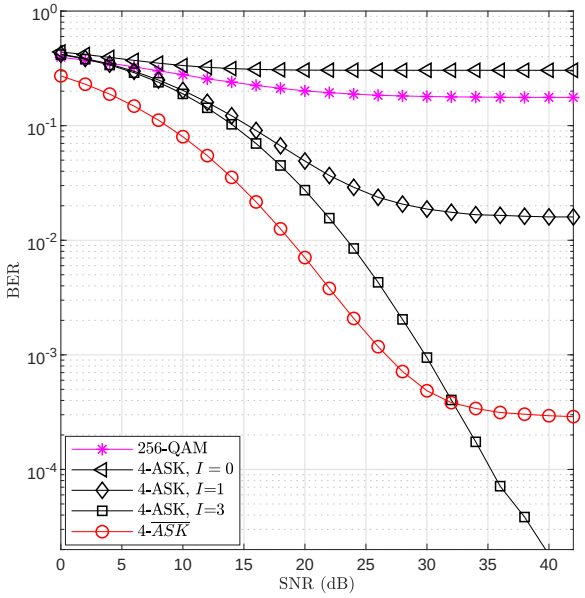

Fig. 3. The comparison between the BER of ASK with PAPR reduction using different number of iterations, compared to the $\overline{\text{ASK}}$ and QAM without PAPR reduction, the positive clipping factor $\mu_c = 1.5$.

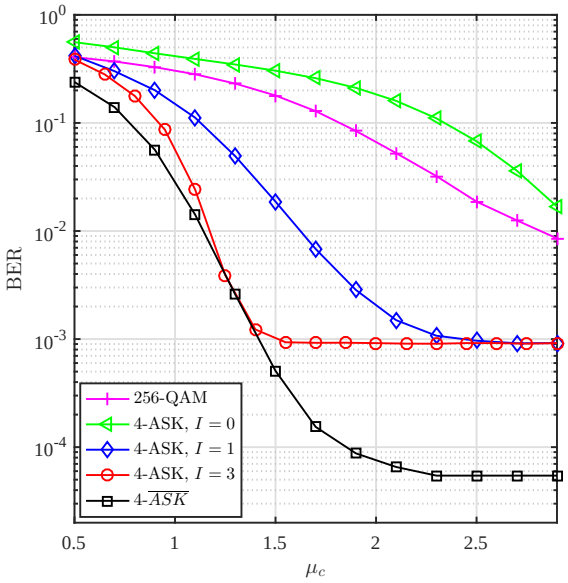

Fig. 4. The effect of the clipping factor μ_c on the BER, SNR $=$ 30 and $M = 4$.

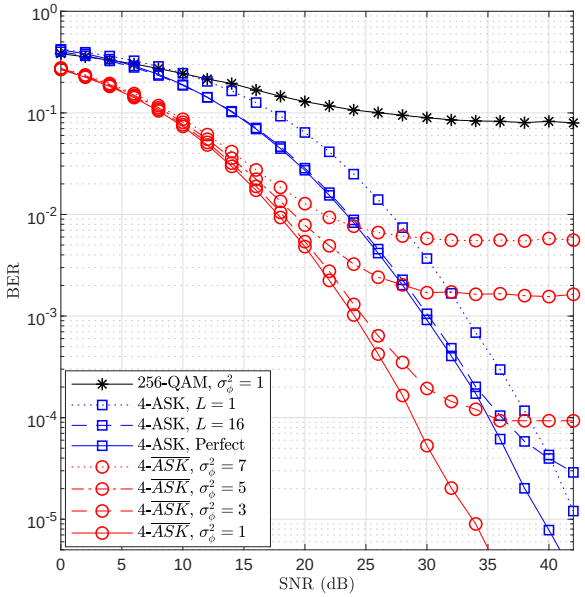

Fig. 5. The effect of phase noise on the considered detection mehods for different values of phase noise variance σ_ϕ^2, $M = 4$, and no clipping.

clipping, and thus, an error floor starts to appear for SNR $>$ 35 dB. The impact of PAPR reduction on ASK is demonstrated for $I = 1$ and 3, where the case of $I = 1$ shows some improvement, but an error floor can still be observed at BER of $\sim 1.8 \times 10^{-2}$. It is also worth noting that the PAPR using $I = 1$ is similar to the 4-$\overline{\text{ASK}}$, nevertheless, the 4-$\overline{\text{ASK}}$ has better BER because it is less sensitive to ICI. Using $I = 3$ with the 4-ASK managed to eliminate the error floor, and thus, outperforms the 4-$\overline{\text{ASK}}$ at high SNRs.

Fig. 4 shows the BER versus the clipping level μ_c where SNR $=$ 30 dB and using $\mathbf{m}_2$ scenario. The SNR is generally selected high so that the performance is mostly determined by the ICI. As can be noted from the figure, using low clipping values deteriorates the BER for all schemes significantly. However, the 4-ASK with $I = 0$ and 256-QAM are the most sensitive to the clipping level. The 4-ASK using $I = 3$ and 4-$\overline{\text{ASK}}$ exhibit equivalent BER for $\mu_c \sim 1.3$ because the 4-$\overline{\text{ASK}}$ does not use PAPR reduction. The BER of the 4-ASK using $I = 3$ becomes independent of the clipping for $\mu_c \gtrsim 1.6$, while it is about 2.3 for the 4-$\overline{\text{ASK}}$ case. It is worth noting that the 4-ASK outperforms the 4-$\overline{\text{ASK}}$ for SNR $>$ 30 dB when for $\mu_c \sim 1.3$, the results are omitted to avoid crowding the figure.

Fig. 5 shows the effect of the phase noise on the considered detection schemes using $\mathbf{m}_2$. The phase noise is modeled as a Tikhonov random variable with variance $\sigma_\phi^2 = [1^\circ, 3^\circ, 5^\circ, 7^\circ]$. The BER of the ASK is represented by a single curve because AC detection is immune to phase noise. The BER for the 256-QAM is presented only for $\sigma_\phi^2 = 1^\circ$ because the BER deteriorates significantly even for such low phase noise scenarios. The 4-$\overline{\text{ASK}}$ is more immune than the 256-QAM, yet there is a significant degradation for $\sigma_\phi^2 \geq 5^\circ$. The figure also shows the ASK performance using the proposed blind channel estimation. As can be noted from the figure, using $L = 16$ is sufficient to provide near-optimal BER for SNR $\lesssim$ 33 dB while using $L = 1$ caused a 3 dB BER degradation. At SNR $\approx$ 40 dB, using $L = 1$ provides more accurate channel estimates because the $L = 16$ case may consist of data symbols with the incorrect constellation point, which implies that L should be selected dynamically based on the system and channel parameters.

VI. Conclusion

This paper presented the design and performance evaluation of an OFDM based OWC system using AC detection. By exploiting the facts that AC detection requires real data at the transmitter, and it does not require phase information at the receiver, an efficient transmitter/receiver design with PAPR reduction and channel estimation techniques was proposed. The modulator was designed using the IDCT, and hence the Hermitian symmetry constraint was omitted, which improved the spectral efficiency of the system. The proposed PAPR reduction algorithm starts by randomly changing the phase of the transmitted data sequence, and then improve the PAPR iteratively. Consequently, the algorithm complexity was minimized, and no mapping information should be exchanged between the transmitter and receiver. The complexity analysis and simulation results confirmed the efficiency of the proposed PAPR reduction algorithm. The proposed channel estimation algorithm resorted to the flatness of the OWC channel to recognize the symbols with the maximum modulation orders, and used them as virtual pilots. Consequently, the channel estimates were obtained using a large number of virtual pilots, which provided near perfect CSI. The BER of the proposed system was evaluated and compared to other OFDM based systems using coherent detection in the presence of phase noise, and the obtained results confirmed the robustness of the AC detector. Consequently, integrating AC detection with OWC has several desirable features as compared to conventional detection schemes.

References

[1] S. Xiaobin, *et al.*, "71-Mbit/s ultraviolet-B LED communication link based on 8-QAM-OFDM modulation," *Opt. Express*, vol. 25, no. 19, pp. 23267-23274, 2017.

[2] D. Tsonev, *et al.*, "A 3-Gb/s single-LED OFDM-based wireless VLC link using a Gallium nitride μLED," *IEEE Photon. Technol. Lett.*, vol. 26, no. 7, pp. 637-40, Apr. 2014.

[3] M. Esmail, A. Ragheb, H. Fathallah, and M. Alouini, "Experimental demonstration of outdoor 2.2 Tbps super-channel FSO transmission system," *IEEE Int. Conf. Commun*. (ICC), 2016, pp. 169-174.
[4] J. Puschell and R. Bayse, "High data rate ultraviolet communication systems for the tactical battlefield," *Proc. of Tactical Communications Conf.*, pp. 253–267, 1990.
[5] M. Khalighi and M. Uysal, "Survey on free space optical communication: a communication theory perspective," *IEEE Commun. Surveys Tuts.*, vol. 16, no. 4, Fourth Quarter, 2014.
[6] J. Armstrong, "OFDM for optical communications," *J. Lightw. Technol.*, vol. 27, no. 3, pp. 189-204, Feb. 2009.
[7] S. Dissanayake and J. Armstrong, "Comparison of ACO-OFDM, DCO-OFDM and ADO-OFDM in IM/DD systems," *J. Lightw. Technol.*, vol. 31, no. 7, pp. 1063-72, Apr. 2013.
[8] M. Uysal *et al*., "IEEE 802.15. 7r1 reference channel models for visible light communications," *IEEE Commun. Mag.*, vol. 55, no. 1, pp. 212-217, Jan. 2017.
[9] M. Obeed, A. Salhab, M. Alouini, and S. Zummo, "On optimizing VLC networks for downlink multi-user transmission: A survey," *IEEE Commun. Surveys Tuts*., vol. 21, no. 3, pp. 2947-2976, thirdquarter 2019.
[10] X. Yi *et al*., "Phase noise effects on phase-modulated coherent optical OFDM," *IEEE Photon J.*, vol. 8, pp. 1-8, Feb. 2016.
[11] M. Al-Jarrah, K. Park, A. Al-Dweik and M. Alouini, "Error rate analysis of amplitude-coherent detection over Rician fading channels with receiver diversity," *IEEE Trans. Wireless Commun*., *IEEE early access*, doi: 10.1109/TWC.2019.2942588, Oct. 2019.
[12] A. Al-Dweik and Y. Iraqi, "Error probability analysis and applications of amplitude-coherent detection in flat Rayleigh fading channels," *IEEE Trans. Commun.*, vol. 64, no. 5, pp. 2235-2244, May 2016.
[13] L. Bariah *et al*., "Performance analysis of semi-coherent OFDM systems with imperfect channel estimates," *IEEE Trans. Veh. Technol.*, vol. 67, no. 11, pp. 10773-10787, Nov. 2018.
[14] J. Zhou, Y. Qiao, Z. Cai, and Y. Ji, "Asymmetrically clipped optical fast OFDM based on discrete cosine transform for IM/DD systems," *J. Lightw. Technol.*, vol. 33, no. 9, pp. 1920-1927, May, 2015.
[15] F. Xiong, "M-ary amplitude shift keying OFDM system," *IEEE Trans. Commun.*, vol. 51, no. 10, pp. 1638-1642, Oct. 2003.

BIOGRAPHIES

Mohammad A. Al-Jarrah received his MSc. degree in Electrical Engineering/Wireless Communications from Jordan University of Science and Technology (JUST), 2011. He is currently with the Department of Electrical and Computer Engineering, Khalifa University, United Arab Emirates. His research interest includes distributed decision fusion systems, statistical signal processing, target tracking in RFID networks, and cooperative spectrum sensing.

Ki-Hong Park received the B.Sc. degree in electrical, electronic, and radio engineering from Korea University, Seoul, Korea, in 2005 and the joint M.S. and Ph.D. degrees from the School of Electrical Engineering, Korea University, Seoul, Korea, in 2011. He joined King Abdullah University of Science and Technology (KAUST) as a post-doctoral fellow in April, 2011. Since December 2014, he has been working as a Research Scientist of Electrical Engineering in the Division of Computer, Electrical, Mathematical Science and Engineering (CEMSE). His research interests are in communication theory and its application to the design and performance evaluation of wireless communication systems, underwater visible light communication, optical wireless communications, unmanned aerial vehicle communication and physical layer secrecy.

Arafat Al-Dweik (S'97–M'01–SM'04) received the Ph.D. (Magna Cum Laude) degree in electrical engineering from Cleveland State University, Cleveland, OH, USA in 2001. He was with Efficient Channel Coding, Inc., Cleveland-Ohio, from 1999 to 2001. From 2001 to 2003, he was the Head of Department of Information Technology at the Arab American University in Palestine. Since 2003, he is with the Department of ECE, Khalifa University, United Arab Emirates. He joined University of Guelph, ON, Canada, as an Associate Professor from 2013-2014. He serves as an Editor with the IEEE Transactions on Vehicular Technology and the IET Communications.

Mohamed-Slim Alouini (S'94, M'98, SM'03, F'09) received the Ph.D. degree in electrical engineering from the California Institute of Technology (Caltech), Pasadena, CA, USA, in 1998. He served as a faculty member at the University of Minnesota, Minneapolis, MN, USA, then at Texas A&M University at Qatar, Education City, Doha, Qatar, before joining King Abdullah University of Science and Technology (KAUST), Thuwal, Makkah Province, Saudi Arabia, as a professor of electrical engineering in 2009. His current research interests include the modeling, design, and performance analysis of wireless communication systems.